Radio Science, Volume 19, Number 1, Pages 319–324, January–February 1984

Attenuation rates of coastal radar signals at 25 MHz

R. S. Lyons

Wave Propagation Laboratory, NOAA/ERL

D. E. Barrick

Ocean Surface Research, Inc.

(Received July 11, 1983; revised September 22, 1983; accepted September 22, 1983.)

The attenuation rate of the ground wave signal with range is a factor limiting the performance of coastal radars. We show that observed attenuation rates are less than theoretically predicted rates at 25 MHz. This result, contrary to earlier findings at lower frequencies, suggests the onset of tropospheric ducting above 20 MHz. The attenuation rates for various sea states and distances are tabulated to allow estimates of system performance near 25 MHz.

INTRODUCTION

Use of the frequency region near 25 MHz by coastal radars (called CODAR's) that monitor ocean wave height directional spectra and surface current fields is increasing rapidly. These radars, having compact antennas that transmit and receive vertically polarized fields in a ground wave propagation mode, extract ocean surface information from the Doppler signature of the moving surface [*Barrick et al.*, 1977; *Lipa and Barrick*, 1982]. At present, several groups (both within and outside the United States) have procured CODAR systems, and frequencies near 25 MHz have been officially allocated for CODAR use.

Essential to predicting and understanding system performance is a knowledge of how rapidly the sea echo signal attenuates with range. This attenuation rate dictates how far useful sea surface information can be obtained. Although asymptotic solutions to the problem of propagation near a smooth spherical earth date back to *Watson* [1918, 1919], simplifications of the solutions suitable for numerical calculations are found in the works by *Wait* [1962] and *Fock* [1965]; *Berry and Chrisman* [1966] have written FORTRAN computer programs that calculate these propagation losses. *Barrick* [1970, 1971*a*, *b*] studied the effect of roughness, or "sea state," on propagation loss above an otherwise smooth sea and found that it could be included at MF/HF as an alteration of the effective surface impedance (or conductivity and dielectric constant) of the ocean. *Barrick and Evans* [1976] used these results to show that a CODAR system radiating 100 W average power should obtain useful sea echoes out to 60–70 km. Many field experiments since then have shown considerable variation in maximum useful range, but more often than not, range has been short of 60 km.

There are two meaningful ways to define the attenuation rate, both in decibels per kilometer; we employ both here. The first defines the rate as proportional to the negative rate of change of the actual received signal power with range R for a ground wave sea scatter radar, assuming statistically homogeneous wave and echo properties with range at a given bearing. The second way removes the $1/R^3$ dependence of the received signal power, characteristic of surface scatter and free-space two-way attenuation. This latter quantity is therefore twice the one-way attenuation rate (also in decibels per kilometer) inherent in the "Norton attenuation factor," F, used by *Wait* [1962] and others. Attenuation rate according to the second definition is also expected to approach a constant value for ground waves over a spherical earth at great distances.

Recent, careful analyses of experimental radar data [*Forget et al.*, 1982] at 7 and 14 MHz have shown that propagation loss at these frequencies follows the theoretical results of *Barrick* [1971*a*, *b*] closely, indicating a clear dependence on sea state. Our experience at 25 MHz also shows pronounced sea state

Paper number 3S1557.
0048-6604/84/003S-1557$08.00

effects: in higher seas, maximum range is decreased. *Forget et al.* [1982] found that measured attenuation rates were slightly greater than theory predicted. Unpublished measurements of one-way path loss over the ocean off the coast of Maine (taken on many frequencies from 3 to 30 MHz 15 years ago by the second author) also show close agreement with theoretical values at frequencies below about 20 MHz, but a consistent trend toward lower losses than predicted above 20 MHz. *Hansen* [1977] found exactly the same behavior over a 235-km path off southern California from 4 to 32 MHz; because his measurements were taken at a fixed path length, it is not possible to determine the rate of change of loss with distance necessary for radar applications. *Pappert and Goodhart* [1979] demonstrated using Hansen's measurements and radiosonde atmospheric data that the decreased loss above 20 MHz can be explained by tropospheric ducting.

We present here sample measurements taken over a 5-day period with the CODAR crossed-loop system in 1980 [*Barrick and Lipa*, 1979; *Lipa and Barrick*, 1982]. Obtained at North Carolina looking eastward into the Atlantic during ARSLOE (Atlantic Remote Sensing Land/Ocean Experiment), this data sample spans a fairly intense storm. Wave conditions ranged between calm and 5 m (significant wave height), and atmospheric conditions from sunny to heavy rain. We have computed the attenuation (or loss) rate over the sea (in decibels per kilometer) to compare with theoretical results. Because of the way the system operates, we were able to obtain only rates, not absolute attenuations.

EMPIRICAL METHODS

The ARSLOE tests took place during October and November 1980 near Duck, North Carolina (36°13′20″N; 75°46′12″W). The CODAR system transmitted on an omnidirectional antenna and received simultaneously on three elements: two electrically small crossed loops having cosine-squared power patterns and an omnidirectional element [*Lipa and Barrick*, 1982]. The loop maxima were pointed $\pm 45°$ with respect to the perpendicular to the straight coastline (i.e., 25°T for antenna 1 and 115°T for antenna 2; antenna 3 is omnidirectional). Both antennas were located near the water, with the heights of their phase centers within a quarter wavelength of sea level. The sea echo time series were recorded on magnetic tape for 32 range cells spaced 1.2 km apart. Each time series is 36 min long. Using a standard fast Fourier transform on the time series for each antenna and range cell, we obtain the power Doppler spectrum. Signal-to-noise ratio (snr) is defined as the ratio of the average of 10 power spectral points around the maximum echo spectral peak to an average of 100 points at the edges of the spectral window; the signal at these positions is known to be external atmospheric noise. The snr's (converted to decibels) from eight 1024-point transforms 4.5 min long are calculated for the 36-min data run. An average of the snr at each range was calculated from the eight samples, along with the associated variance. The study is confined to ranges from 23.4 to 30.6 km from the radar; the automatic gain controls and other signal normalization procedures in the system destroy the relative snr variation with range at closer ranges, and the farther ranges were omitted because the snr there is sometimes too small for reliable use.

THEORETICAL MODEL USED

A model for the received signal strength has been postulated and employed to calculate expected average signal power loss rate (versus range) for the antenna elements used in this system. The received signal power strength is an angular integral of the sea echo within a semicircular range cell weighted by the antenna patterns for each of the three receiving antenna elements. The sea echo and the propagation loss appearing as factors in the integrand are also functions of azimuth angle. The first-order sea echo is directly proportional to the ocean wave height directional spectrum at 6-m wavelength, in the azimuth direction of interest. We employ a Joint North Sea Wave Project (JONSWAP) model [*Hasselmann et al.*, 1976] that also incorporates a directional factor [*Hasselmann et al.*, 1980]. This wind wave model is a function of three parameters that we obtain from environmental measurements by others at ARSLOE: wind speed (or wave height) and direction, and a development factor. The latter depends on duration (the period over which the wind has been blowing) and fetch (the distance over which the wind has been blowing). In all cases the wind was sufficient that the 6-m waves that produced the sea echo were "saturated," i.e., developed to their maximum possible height for the given fetch; the directional pattern of the sea echo according to this model therefore was very broad. The strength of the JONSWAP spectrum in the saturated region is described by the constant α (to which the first-order sea echo is directly proportional); this constant is shown to be a weak func-

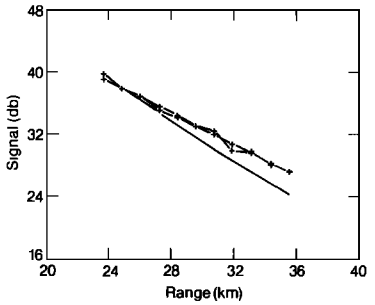

Fig. 1. Signal-to-noise ratios with weighted regression line (the lines with pluses) as well as theoretical signal strength adjusted to the first data value are plotted versus range from the radar site for the omnidirectional antenna at 0930 UT on October 23, 1980.

tion of fetch [*Hasselmann et al.*, 1976]. Only the last time period we examined, when the wind was offshore, contains the possibility that the sea echo might therefore vary with range from the radar. Because of the small range interval studied here (23.4–30.6 km) and the weak dependence of α on fetch, its variation (and hence that of the first-order radar cross section) across this interval is less than 3%, and therefore we neglect it.

The propagation loss to a point in the range cell depends on the effective surface impedance, which is a function of the sea state, i.e., the wave height directional spectrum; the propagation loss was shown [*Barrick*, 1971*a*, *b*] to be only slightly directionally dependent. We used a surface impedance that included the effects of swell (i.e., nearly sinusoidal waves from a distant storm), along with the wind waves. Swell, when present, was estimated from the National Oceanic and Atmospheric Administration (NOAA) pitch/roll buoy operating in the area. Wind waves were estimated from the same JONSWAP wind wave model mentioned above. Using these estimates of surface impedance to account for the sea surface conditions occurring at the time of each measurement, we calculated the propagation loss to the given range at the specific integration angle with the FORTRAN program of *Berry and Chrisman* [1966]. The integration over angle for each antenna then gave the predicted signal power strength as a function of range, except for an unknown multiplicative constant containing system gains. The attenuation "rate" in decibels per kilometer (a logarithmic function that eliminates multiplicative factors) was therefore calculated from this model. An example of this theoretical loss is the unmarked curve in Figure 1.

Results of these theoretical calculations show that attenuation rate does not exhibit a directional dependence. That is, different directional patterns showed no appreciable differences in loss rates. This is undoubtedly due to the broad-beam antenna patterns and also to the only slight directional dependence of the propagation loss at 25 MHz, as shown by *Barrick* [1970, 1971*a*, *b*].

Finally, we employed the simplest possible model to examine tropospheric refractivity effects: modification of the effective earth radius factor in the ground wave loss calculations, based on different lapse rates of refractivity near the surface [*Wait*, 1962; *Bean*, 1964]. The latter shows from extensive measurements over all parts of the earth in all weather conditions that the total possible span of (average) refractivity lapse, ΔN, in the lowest kilometer varies between -20 and -80. Effective earth radius factors corresponding to this span go from 1.2 to 2.0 (in comparison with the $\frac{4}{3}$ factor normally used). Employing these extremes in the loss calculations produced no appreciable change in the attenuation rates, at least not enough to explain the differences observed experimentally. Hence we conclude that differences observed, if they are indeed due to atmospheric effects, cannot be explained by this simple, one-parameter refractivity model. Although much more complicated models have been postulated for ducting [*Fock*, 1965] and applied at HF [*Pappert and Goodhart*, 1979], it did not appear worthwhile to do the involved loss calculations since (1) no detailed measurements of the duct refractivity profile were available at ARSLOE in the CODAR coverage area and (2) forcing the output of a multiparameter model to fit one data point (i.e., the loss rate at a given time) would produce no credible conclusions as to tropospheric effects on path loss.

COMPARISONS

We now compare the theoretical and observed attenuation rates with range (measured in decibels per kilometer) at 25.4 MHz for many sea state conditions. The radar cross section of the sea is taken to be constant with distance over the sea state conditions and range interval considered here (see justification of preceding section); therefore the received signal strength, or snr, is a direct measure of the path loss. The observed path attenuation rates are calculated from eight independent sea echo spectra at each radar range; thus 48 independent data values determine the attenuation rate for each antenna. Attenuation rates are then obtained at five different times

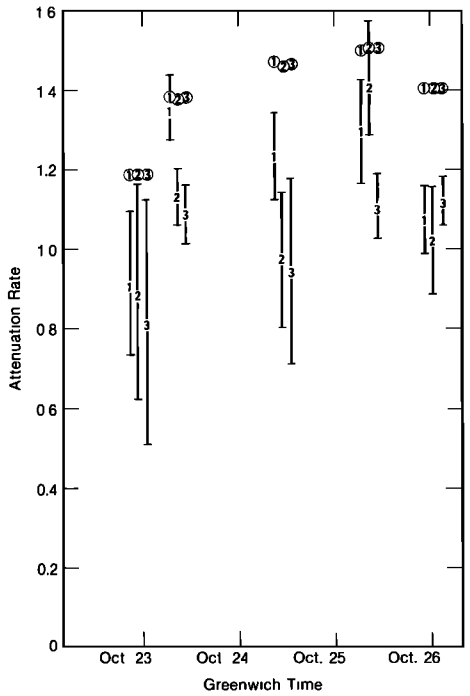

Fig. 2. Theoretical and actual attenuation rates for received signal power (in decibels per kilometer) for receiving antennas 1, 2, and 3 at five different times. Circled antenna numbers denote theoretical rates. Antenna 1 is $+45°$ from perpendicular to coast, and antenna 2 is $-45°$; both have cosine-squared antenna patterns. Antenna 3 is omnidirectional. The uncertainties for the theoretical attenuation rates were so small that they were omitted.

during the storm, spanning various sea states. The corresponding theoretical attenuation rates are calculated for the same sea state conditions and over the same range interval (23.4–30.6 km).

Unknown multiplicative power factors for both theoretical and experimental results thus become additive quantities, or intercepts, when converted to decibels; hence they can be matched at one point, as done by *Forget et al.* [1982]. As an example of the snr comparisons between data and theory, Figure 1 shows the observed value and its regression line (calculated in a least squares sense but weighted by the variances at each range); both are marked by pluses. The theoretical signal strength is shown as the solid curve, matched to the data at the first point; this example is the omnidirectional antenna (antenna 3) on October 23 at 0930 GMT. Since the theoretical line has a larger negative slope for the 11 ranges shown, its attenuation rate is slightly greater than the measured rate. This is a typical example of actual data and theoretical values. For all other times and antennas, theoretical falloff rates are always greater than observed values, as shown in Figure 2. The theoretical attenuation rates over the range interval (23.4–30.6 km) in Figure 2 are all larger than the measured rates for all times studied.

Preceding the storm on October 22, significant wave heights were 0.5 m, as measured by the NOAA XERB data buoy in the area. As the storm intensified, the wave height increased to 1.7 m on October 24; winds/waves were from the northeast. The peak of the storm on October 25 saw wave heights of 4.5 m. As the storm abated, wave heights decreased to 1.7 m on October 26, but the winds were blowing from the west, generating a second set of shorter-period, offshore waves of lower height. During the period when the wave height was increasing, we observed that the absolute snr decreased for a given range, as evidenced by the decrease in maximum usable range of the system.

For 25.4 MHz at a mean range of 26 km, Figure 2 shows that the attenuation rate is a clear function of sea state; in the cases of both theory and experiment, the attenuation rate increases with increasing wave height. The error bars on the measured data points in Figure 2 and the uncertainties given in Table 1 are determined by the regression coefficient for the fit of snr to range; use is then made of the T statistic for 95% confidence with $N - 2$ degrees of freedom, where N is the number of points employed in the regression fit. (In this case, $N = 6$.) Variances were determined for a regression fit to the theoretical curves. The variances in this case represent the deviation of the curve from a straight line; associated error bars are always smaller than 0.025 and are not shown. Figure 2 uses the first definition of attenuation rate, i.e., the falloff of the actual received sea echo power. Table 1 gives values according to both definitions; *Forget et al.* [1982] presented their results using the second definition, i.e., with range-cubed effects removed.

The results here show an opposite relation between theory and experiment from results of others at lower HF. *Forget et al.* [1982] observe a greater attenuation with range at 7 and 14 MHz than predicted by theory, for various wind/wave conditions. Although *Forget et al.* [1982] used theoretical curves of *Barrick* [1970] based on different wave spectral models from the JONSWAP employed here (i.e., a Neuman-Pierson and a Phillips model), we observe in fact that the shape of the spectral model used to calculate the loss curves has almost no effect on the loss rates at 25 MHz; hence this does not explain the differences.

TABLE 1. Observed and Theoretical Attenuation Rates With Uncertainties, by Time and Antenna, for Received Signal Power and Received Signal With Range-Cubed Effects Removed

			Rate According to Data, dB/km		Rate According to Theory, dB/km	
Day	Time	Antenna	Power	Power × R^3	Power	Power × R^3
Oct. 22	2330	1	0.9119 ± 0.1903	0.4166 ± 0.3743	1.1863 ± 0.0164	0.6911 ± 0.0151
		2	0.8881 ± 0.2821	0.3929 ± 0.5229	1.1940 ± 0.0167	0.6988 ± 0.0194
		3	0.8071 ± 0.3084	0.3119 ± 0.6012	1.1917 ± 0.0145	0.6964 ± 0.0081
Oct. 23	0930	1	1.3517 ± 0.0888	0.8572 ± 0.1297	1.3817 ± 0.0164	0.8864 ± 0.0030
		2	1.1329 ± 0.0895	0.6424 ± 0.1548	1.3731 ± 0.0162	0.8779 ± 0.0073
		3	1.0894 ± 0.0908	0.6054 ± 0.1505	1.3776 ± 0.0150	0.8824 ± 0.0096
Oct. 24	0930	1	1.2343 ± 0.1120	0.7318 ± 0.1927	1.4690 ± 0.0194	0.9738 ± 0.0187
		2	0.9750 ± 0.1770	0.4828 ± 0.3529	1.4600 ± 0.0192	0.9647 ± 0.0141
		3	0.9509 ± 0.2308	0.4491 ± 0.4512	1.4645 ± 0.0195	0.9693 ± 0.0120
Oct. 25	0930	1	1.2942 ± 0.1310	0.7958 ± 0.2081	1.4986 ± 0.0215	1.0034 ± 0.0171
		2	1.4038 ± 0.1610	0.9115 ± 0.2404	1.5062 ± 0.0243	1.0109 ± 0.0243
		3	1.1004 ± 0.0863	0.6067 ± 0.1553	1.5036 ± 0.0233	1.0083 ± 0.0180
Oct. 26	0130	1	1.0780 ± 0.0894	0.5791 ± 0.1627	1.3981 ± 0.0166	0.9028 ± 0.0072
		2	1.0224 ± 0.1448	0.5256 ± 0.2683	1.4014 ± 0.0164	0.9062 ± 0.0082
		3	1.1204 ± 0.0669	0.6234 ± 0.1088	1.4007 ± 0.0160	0.9054 ± 0.0132

This study was limited to distances less than 30 km from the radar in order to ensure a high-quality snr. Theoretically, however, attenuation rates at greater distances can be calculated to extend the utility of our findings at 25 MHz. This was done for distances centered on 40, 50, and 60 km, based on calculated values at eight points around these centers. The theoretical values of the attenuation rates at these ranges, according to our two definitions, are presented in Table 2. The attenuation rates are seen to decrease with greater range, possibly approaching an asymptote far out. We go out here only as far as 60 km because this is near the limit for practical sea scatter radars in a ground wave mode at 25 MHz. In obtaining these numbers, we varied the sea states widely (i.e., both wave height and direction), but found very little effect with sea state at these greater ranges; the scatter due to sea state is represented as uncertainties in the table. *Barrick*'s [1970] curves also show insignificant effect of sea state on attenuation rates at 25 MHz at greater ranges, although the absolute power received drops significantly in higher seas (as we observed), with two-way path losses between 10 and 20 dB greater in higher seas (e.g., up to 8 m significant wave height) at ranges beyond 20 km.

CONCLUSIONS

The attenuation rates relative to radar range are important in understanding CODAR's capabilities. We tabulate measured and theoretical attenuation rates with their uncertainties for sea states represented by significant wave heights between 0.5 m and 4.5 m for ranges 23–31 km from shore. These attenuation rates show no directional dependence for three broad-beam receiving antennas (with two loop patterns perpendicular to each other), although the wave directions varied widely over our observation period. These attenuation rates do show a sea state dependence for both ways of defining loss rate. In both cases, measured values are slightly smaller than theoretical rates, contrary to results at lower frequencies. Future experiments should be designed with adequate meteorological sensors to allow identification of the atmospheric conditions responsible for these reduced attenuation rates. Numerical studies of HF tropospheric ducting over the sea [*Pappert and Goodhart*, 1979] indicate, surprisingly, that sharp inversion layers produce less of a propagation enhancement effect than a well-mixed, uniform boundary layer that gives rise to superrefractive conditions; the latter are more typical of the windy ARSLOE storm situation.

TABLE 2. Theoretical Attenuation Rates With Uncertainties (With and Without Range-Cubed Effects), for Distances Beyond the Maximum CODAR Range at ARSLOE

Distance From Radar, km	Rate for Power Received, dB/km	Rate for Power × R^3, dB/km
40.8	1.00 ± 0.05	0.68 ± 0.05
50.4	0.87 ± 0.02	0.61 ± 0.02
60.0	0.76 ± 0.02	0.54 ± 0.02

Theoretical attenuation rates have also been presented for radar ranges of 40, 50, and 60 km as a guide for assessing maximum range capabilities for CODAR users. Observed rates tended to be slightly less than theoretical rates at closer ranges; this trend might be expected to hold at greater ranges also. Tabulated uncertainties represent total variations over all three antennas and for a wide range of sea states. Sea state tends to affect the rate less at greater distances, although our measurements show a drop in absolute signal strength.

REFERENCES

Barrick, D. E., Theory of ground-wave propoagation across a rough sea at dekameter wavelengths, research report, Battelle Mem. Inst., Columbus, Ohio, 1970.

Barrick, D. E., Theory of HF and VHF propagation across the rough sea, 1, The effective surface impedance for a slightly rough highly conducting medium at grazing incidence, *Radio Sci.*, *6*, 517–526, 1971*a*.

Barrick, D. E., Theory of HF and VHF propagation across the rough sea, 2, Application to HF and VHF propagation above the sea, *Radio Sci.*, *6*, 527–533, 1971*b*.

Barrick, D. E., and M. W. Evans, Implementation of coastal current-mapping HF radar system: Progress report no. 1, *NOAA Tech. Rep. ERL 373-WPL 47*, Environ. Res. Lab., U.S. Dep. of Commerce, Boulder, Colo., 1976.

Barrick, D. E., and B. J. Lipa, A compact transportable HF radar system for directional wave field measurements, in *Ocean Wave Climate*, edited by M. D. Earle and A. Malahoff, pp. 153–201, Plenum, New York, 1979.

Barrick, D. E., M. W. Evans, and B. L. Weber, Ocean surface currents mapped by radar, *Science*, *198*, 138–144, 1977.

Bean, B. R., Tropospheric refraction, in *Advances in Radio Research*, edited by J. A. Saxton, pp. 53–120, Academic, New York, 1964.

Berry, L. A., and M. E. Chrisman, A FORTRAN program for calculation of ground wave propagation over homogeneous spherical earth for dipole antennas, *Rep. 9178*, Natl. Bur. of Stand., U.S. Dep. of Commerce, Boulder, Colo., 1966.

Fock, V. A., *Electromagnetic Diffraction and Propagation Problems*, Pergamon, New York, 1965.

Forget, P., P. Broche, and J. C. de Maistre, Attenuation with distance and wind speed of HF surface waves over the ocean, *Radio Sci.*, *17*, 599–610, 1982.

Hansen, P., Measurements of basic transmission loss for HF ground wave propagation over sea water, *Radio Sci.*, *12*, 397–404, 1977.

Hasselmann, K., D. B. Ross, P. Muller, and W. Sell, A parametric wave prediction model, *J. Phys. Oceanogr.*, *6*, 200–228, 1976.

Hasselmann, D., M. Dunckel, and J. A. Ewing, Directional wave spectra observed during JONSWAP 1973, *J. Phys. Oceanogr.*, *10*, 1264–1280, 1980.

Lipa, B. J., and D. E. Barrick, CODAR measurements of ocean surface parameters at ARSLOE—Preliminary results, paper presented at Oceans '82 Conference, Inst. of Electr. and Electron. Eng., Washington, D. C., 1982.

Pappert, R. A., and C. L. Goodhart, A numerical study of tropospheric ducting at HF, *Radio Sci.*, *14*, 803–813, 1979.

Wait, J. R., *Electromagnetic Waves in Stratified Media*, Pergamon, New York, 1962.

Watson, G. N., The diffraction of radio waves by the earth, *Proc. R. Soc. London, Ser. A*, *95*, 83–99, 1918.

Watson, G. N., The transmission of electric waves around the earth, *Proc. R. Soc. London, Ser. A*, *95*, 546–563, 1919.

D. E. Barrick, Ocean Surface Research, Inc., 1131 Cranbrook Court, Boulder, CO 80303.

R. S. Lyons, Wave Propagation Laboratory, NOAA/ERL, Boulder, CO 80303.